

**HELLENIC NUCLEAR PHYSICS SOCIETY**

**PROCEEDINGS**

**25<sup>th</sup> HELLENIC CONFERENCE**

**ON**

**NUCLEAR PHYSICS**



**NATIONAL CENTRE FOR SCIENTIFIC RESEARCH  
“DEMOKRITOS”**

**3 & 4 JUNE 2016**

# TABLE OF CONTENTS

<b>Theo Zouros</b> Atomic Physics with Accelerators: Projectile Electron Spectroscopy of highly charged ions at the 5.5MV Demokritos Tandem accelerator	1
<b>Maria Zamani</b> Triple fission events at high energies	16
<b>Charalambos Moustakidis</b> Speed of Sound Effects on the Upper Bound of Neutron Star Mass	22
<b>George Koutelieris</b> Gas System for the ATLAS NSW Micromegas Detectors: Design Aspects and Advanced Validation Methods for their QA/QC	23
<b>Nikolas Patronis</b> Study of the $^{193}\text{Ir}(n,2n)^{192}\text{Ir}$ Reaction Cross Section	29
<b>Panagiotis Gastis</b> Nuclear reaction studies for the vp-process	35
<b>Anastasios Lagogiannis</b> Benchmarking cross sections for PIGE: The Fluorine case	36
<b>Aggeliki Assimakopoulou</b> Systematic Study of proton-induced spallation reactions with the Constrained Molecular Dynamics (CoMD) Model	42
<b>George Apostolopoulos</b> Interactions between carbon impurities and defects produced by proton irradiation in $\alpha$ -iron	47
<b>Anastasia Savidou</b> Activities and prospects of the radioactive materials management laboratory at NCSR "Demokritos"	53
<b>Theodora Vasilopoulou</b> Preparation of activation experiments for ITER material characterization and data validation in the Deuterium-Tritium JET campaign	59
<b>Nick Gazis</b> Engineering Design Integration & Non-Destructive Testing for the ESS accelerator	65
<b>Eleni Adamidi</b> The EDUSAFE project	72
<b>Kornilios Routsonis</b> Experimental study of the flux trap effect in a sub-critical assembly	79
<b>Basile Spyropoulos</b> Radiotherapy (RT) innovative Technology combined with Hospital/Home-Care Standards and Medical Protocols & Guidelines: A collective Compendium	85
<b>Alexandros Clouvas</b> Periodicity analysis of long period gamma radiation measurements in Thessaloniki, Northern Greece	91
<b>John Kalef-Ezra</b> Limitations in the assessment of radon dose: the role of direct activity measurements	92
<b>Alexandra Ioannidou</b> Activity size distribution of radioactive nuclide $^7\text{Be}$ at different locations and under different meteorological conditions	97
<b>Eleftheria Ioannidou</b> Time lag between the tropopause height and the levels of $^7\text{Be}$ concentrations in surface air	102
<b>Marilia Savva</b> Determination of $^7\text{Be}$ , $^{210}\text{Pb}$ and $^{22}\text{Na}$ Activity in Air and Rainwater samples by Gamma-ray Spectrometry	108
<b>Ekaterinini Dalaka</b> Temporal variations of $^7\text{Be}$ and its AMAD over "Demokritos" GAW station"	116
<b>Roza Vlastou</b> Investigation of $(n,xn)$ reactions using the high energy neutron facility at NCSR "Demokritos"	117
<b>Eleni Vagena</b> Measurement of the average cross section for $^{162}\text{Er}(g, n)$ reaction with bremsstrahlung photons; comparison with theoretical calculations using the TALYS model	123
<b>Veatriki Michalopoulou-Petropoulou</b> A simple angle integration method for the determination of capture reaction cross sections	129

<b>Varvara Lagaki</b>	
Installation of Neoptolemos, the new sum spectrometer for cross section measurements of capture reactions at the Tandem Accelerator Laboratory of NCSR “Demokritos”.	134
<b>Athanasios Stamatopoulos</b>	
The $^{240}\text{Pu}(n,f)$ cross section measurement at the new experimental area at CERN's n_TOF facility	139
<b>Antigoni Kalamara</b>	
$^{197}\text{Au}(n,xn)$ reactions at TSL high energy neutron facility at Uppsala	145
<b>Dimitrios Papoulias</b>	
Probing electromagnetic neutrino properties from neutrino-nucleus scattering	152
<b>Marianthi Fragopoulou</b>	
Space radiation dosimetry	153
<b>Konstantinos Preketes-Sigalas</b>	
Development of a simulation code for material analysis using the PIGE technique	162
<b>Ioannis Tzifas</b>	
Application of Synchrotrons radiation and fission track techniques to the characterization of U-bearing organic rich limestones of NW Greece.	167
<b>Ahmed Khaliel</b>	
Experimental investigations of radiative proton-capture reactions relevant to explosive nucleosynthesis	168
<b>Vasiliki Angelopoulou</b>	
Resurrected from the dead: Full characterization of an old HPGe detector using $\gamma$ -ray and CT tomographies coupled to standard calibration techniques and simulations	174
<b>Ioanna Sfampa</b>	
Correlation between isothermal TL and IRSL in K-feldspars of various Types	182
<b>Christos Tsabaris</b>	
$\gamma$ -ray spectrometry practices in the deep ocean	183
<b>Froso Androulakaki</b>	
Utilization of the Monte Carlo code FLUKA for Applications in the Marine Environment	184
<b>Filothei Pappa</b>	
Comparison of MCNP and ERICA codes in two different marine areas	185
<b>Georgia Mavrokefalou</b>	
Remote radiological assessment in the marine environment: A pilot study based on $^{137}\text{Cs}$ measurements and satellite observations in the Aegean Sea.	191
<b>Georgios Kuburas</b>	
A survey on the radioactivity of mineral springs in Greece	198
<b>Konstantia Valasi</b>	
An autonomous underwater telescope for measuring the scattering of light in the deep sea	199
<b>Kostantinos Eleftheriadis</b>	
Long term measurements of radioactive tracers over “Demokritos GAW station”	205
<b>Georgia Travidou</b>	
The Use of Nuclear Methods and Techniques in Radioecology: Teaching Approaches in the Secondary Education	206
<b>Athanasios Papageorgiou</b>	
Rare Isotope Production in peripheral heavy-ion collisions in the energy range 15-25 MeV/nucleon	207
<b>Nick Gazis</b>	
Engineering, Design Integration and the Integration Test Standard in the Engineering Resources Group	216
<b>Iason Mitsios</b>	
Investigation of natural and anthropogenic radionuclides particle-size dependence in surface soils	217
<b>Maria Sotiropoulou</b>	
Radiological impact assessment in the terrestrial environment of Greece using innovative tools - Adaptation of ERICA Tool to actual measurements	222
<b>John Kalef-Ezra</b>	
Design and operation of a therapeutic unit with unsealed radioactive sources	226
<b>Heleny Florou</b>	
The evolution of $^{137}\text{Cs}$ in the Greek marine environment and dose rate assessment in fish representing the three discrete exposure spaces	230

<b>Sofia Kolovi</b>	
Assessment of the efficiency of iron stain removal treatment in textiles by X-ray fluorescence: Preliminary results	231
<b>Kostoula Triantou</b>	
Positron Annihilation Lifetime Spectroscopy in the Study of Defects in Materials	235
<b>M. Alexandropoulou K. Ioannides</b>	
Validation of the ImageJ package for alpha track counting on Solid State Nuclear Track Detectors	239
<b>Ioannis Madesis</b>	
Evaluation of 1s2l2l' 4P/2P, 2P+/2P- and 2D/2P ratios from collisions of mixed state (1s2, 1s2s 3S) He-like ion beams with H2 and He targets	243
<b>Stefania Dede</b>	
Benchmarking the natSi(p,p0) and natO(d,d0) elastic scattering and the 16O(d,p0,1,α0) reactions for IBA purposes	244
<b>Anastasios Kanellakopoulos</b>	
Neutron-induced fission cross-section measurement of 234U with monoenergetic beams in the keV and MeV range using Micromegas detectors	250
<b>Sofia Papadimitriou</b>	
Microscopic description of neutron-induced fission with the Constrained Molecular Dynamics (CoMD) Model: Preliminary Results	255
<b>Kalliopi Tsampa and E-M Lykiardopoulou</b>	
Construction and Ion-Beam Characterization of Nuclear Targets	258
<b>Dimitrios Papaioannou</b>	
Exploring the feasibility of magnetic moment measurements in the exotic 20C nucleus using LISE++ calculations	262
<b>Angelos Laoutaris</b>	
Installation of a gas terminal stripper and a gas/foil post stripper system at the 5.5 MV Demokritos Tandem Van de Graaff accelerator	266
<b>Argyrios Papadopoulos</b>	
Assessment of gamma radiation exposure and distribution of natural radioactivity in beach sands close to plutonic rocks of Greece	271
<b>Eleni Ntemou</b>	
Measurement of differential cross sections of natLi(d, d0) for EBS purposes	272
<b>Pavlos Tsavalas</b>	
Investigation of the ITER-like wall divertor Tiles at JET tokamak	276
<b>Georgios Eleftheriou</b>	
Towards the development of a radiological box model for Aegean Sea: considerations and perspectives	280
<b>Conference Program</b>	281

**Zero-degree Auger Projectile Electron Spectroscopy of Li-like Ions obtained in Collisions of  $1s2s^3S$  He-like Ions with Gaseous Targets**

I. Madesis,<sup>1,2</sup> A. Laoutaris,<sup>1,2</sup> E. P. Benis,<sup>3</sup> A. Lagoyannis,<sup>2</sup> M. Axiotis,<sup>2</sup> and T. J. M. Zouros<sup>1,2</sup>

<sup>1)</sup>*Department of Physics, University of Crete, P.O Box 2208, GR 71003 Heraklion, Greece*

<sup>2)</sup>*Tandem Accelerator Laboratory, Institute of Nuclear and Particle Physics, NCSR Demokritos, GR 15310 Ag Paraskevi, Greece*

<sup>3)</sup>*Department of Physics, University of Ioannina, GR 45110 Ioannina, Greece*

An experimental station has recently been completed with a beam line dedicated to atomic collision physics at the 5.5 MV TANDEM accelerator laboratory of the Institute of Nuclear and Particle Physics (INPP) at the National Center for Scientific Research (NCSR) “Demokritos” in Athens. A Zero-degree Auger Projectile Spectroscopy (ZAPS) apparatus composed of a single-stage Hemispherical Deflector Analyser (HDA) and a 2-dimensional Position Sensitive Detector (PSD), combined with a doubly differentially pumped gas target has been set up for high resolution studies of electrons emitted from projectile ions at  $\theta = 0^\circ$  with respect to the beam direction in collisions with dilute gas targets. A terminal gas stripper, as well as both a foil and a gas post-stripper, have also been newly installed, enhancing the capabilities of the TANDEM by allowing for the production of more intense, highly charged ion beams, thus complementing and expanding the range of the available energies and charge states of the TANDEM. Using this setup, a systematic isoelectronic investigation of high resolution K-Augur electron spectra emitted from pre-excited ions in collisions with gas targets has been commenced within the APAPES<sup>1-3</sup> initiative. Here, we present some highlights of this program together with recent results. This investigation is expected to lead to a better understanding of electron capture to excited states of the ion beam and in particular the overlooked role of cascade feeding of metastable states contributing to the capture cross sections, recently a field of contested interpretations awaiting further resolution.

PACS numbers: 02.70.-c, 07.81.+a, 32.70.-n, 32.70.Jz, 02.70.Bf, 34.

## I. INTRODUCTION

High resolution Auger projectile electron spectroscopy has become an important tool, over the last few decades, for obtaining information on both the atomic structure and the collision dynamics of multiply excited ions produced in ion-atom collisions<sup>4</sup>. This interest has been generated to a large extent in the fields of thermonuclear fusion, hot plasmas, astrophysics, accelerator technology and basic physics of ion-atom collision dynamics. Our recent APAPES<sup>1</sup> initiative allows for the first investigations of accelerator-based atomic physics in Greece, using the newly completed and now fully operational, innovative electron spectroscopy apparatus<sup>2,3</sup>. Here, we present the basics of the technique, as well as some of our first results on our investigations of electron capture from gas targets using 12 MeV C<sup>4+</sup> ion beams obtained from the negative ion sputter source of the TANDEM and produced using the newly installed terminal gas stripper.

## II. ZERO-DEGREE AUGER PROJECTILE SPECTROSCOPY - KINEMATIC CONSIDERATIONS

High resolution projectile electron spectroscopy refers to the experimental energy- and angular-resolved electron spectroscopic technique in which electrons ejected from a moving emitter (usually a projectile ion beam) are energy analysed and detected at or close to the observation angle  $\theta = 0^\circ$  with respect to the beam direction. This is why this technique is usually referred to as zero-degree Auger projectile spectroscopy (ZAPS). The ZAPS technique mostly refers to high energy resolution ( $< 0.5\%$ ) measurements of electrons with characteristic energies  $\sim 50\text{-}600$  eV such as those emitted in autoionization, Auger, autodetachment, photo-ionization processes and could possibly even include high energy conversion- and beta-electron emission processes in the future. Because these electrons have characteristic energies they carry important atomic structure information such as state energy, binding energy, line width etc. The particular detection angle of  $\theta = 0^\circ$  offers the *optimal* kinematic conditions for attaining the highest possible resolution. Equally important, this technique also allows for the determination of electron production cross sections at the state-selective level, thus providing important information about the dynamics of the projectile atomic reaction processes, as for example single electron capture, a process of primary interest to

the APAPES<sup>1</sup> investigations.

Since the electrons we measure are emitted from fast projectile ions it is important to understand some of the basics of projectile electron kinematics. A detailed analysis can be quite complicated<sup>5</sup>. However, in the case of energetic collisions of few MeV/u or more, projectile ions are scattered through very small angles ( $\sim$ mrads) resulting in negligible energy loss and influence on the projectile trajectory. Thus, a simple velocity vector addition model is sufficient for the determination of most kinematic effects. The velocity  $\mathbf{v}$  of the Auger electron in the laboratory frame is obtained by adding the projectile velocity  $\mathbf{V}_p$  to the velocity  $\mathbf{v}'$  of the electron in the projectile rest frame as shown in Fig. 1. Denoting with prime quantities in the projectile rest frame, the electron kinetic energy  $\varepsilon$  in the laboratory frame can be related to the corresponding rest frame  $\varepsilon'$  as<sup>4</sup>

$$\varepsilon = \frac{1}{2}m\mathbf{v} \cdot \mathbf{v} = \varepsilon' + t_p + 2\sqrt{\varepsilon't_p} \cos \theta' \quad (1a)$$

or its more accurate *relativistic* counterpart

$$\varepsilon = \gamma_p \varepsilon' + t_p + \sqrt{(1 + \gamma')(1 + \gamma_p)\varepsilon't_p} \cos \theta' \quad (1b)$$

$t_p = \frac{m}{M_p}E_p$  is the reduced projectile energy,  $E_p$  and  $M_p$  are the kinetic energy and mass of the projectile respectively, while  $m$  is the electron mass and  $\gamma_p (= 1 + \frac{t_p}{mc^2})$  and  $\gamma' (= 1 + \frac{\varepsilon'}{mc^2})$  are the usual relativistic  $\gamma$ -parameters for electrons with speeds  $V_p$  and  $v'$ , respectively. Both the second and the third term in the equations imply a substantial energy shift from the rest frame energy (the Auger electron energy)  $\varepsilon'$  to either higher or lower laboratory energies  $\varepsilon$  depending on the value of  $\theta'$  which determines whether the resulting laboratory electron speed  $v$  is larger or smaller than the speed of the electron  $v'$  in the projectile rest frame. The third term also introduces a stretching effect of the spectra that can be used experimentally to the advantage of high energy resolution measurements. In addition, for fast emitters, there is a limiting laboratory observation angle  $\theta_{max}$  (see Fig. 1[left]) beyond which no projectile electrons can be observed. Finally, the relativistic effects at a few MeV/u beam energies is just a small, but observable correction (a few hundred meV) to the measured laboratory electron energy  $\varepsilon$  and helps in the more energy accurate calibration and identification of the Auger lines.

For an electron spectrometer with a finite acceptance angle  $\Delta\theta'$  ( $\Delta\theta$  in the lab frame) it

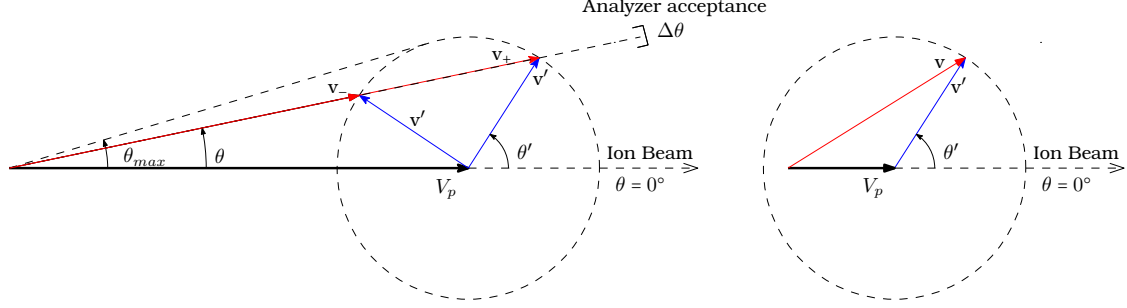


Figure 1. Velocity addition diagrams. The electron velocity  $\mathbf{v}'$  in the projectile rest frame is transformed to the laboratory frame according to the vector addition rule  $\mathbf{v} = \mathbf{V}_p + \mathbf{v}'$ , where  $\mathbf{V}_p$  is the velocity of the projectile emitter. (Left)  $V_p > v'$  leading to a maximum possible laboratory emission angle  $\theta_{max}$ . (Right)  $V_p < v'$ , where all observation angles  $\theta$  are now possible. The ZAPS technique sets the electron analyser at  $\theta = 0^\circ$ , where kinematic broadening effects due to the finite analyser acceptance angle  $\Delta\theta$  are minimized (see text).

is simple to show<sup>4</sup> by direct differentiation of Eq. 1 with respect to  $\theta'$  that:

$$\frac{d\varepsilon}{d\theta'} \propto \sin \theta' \quad (2)$$

where  $\propto$  is the proportionality symbol. This dependence on the *finite* acceptance angle of the spectrometer induces a so called *kinematic broadening* which is a substantial limiting factor at *non-zero* observation angles. However, at the observation angle  $\theta = 0^\circ$  corresponding to  $\theta' = 0^\circ$  or  $180^\circ$ ,  $\frac{d\varepsilon}{d\theta'}$  is zero, implying only second order contributions in  $\Delta\theta'$  or smaller. A simple calculation shows that for a practical electron spectrometer acceptance angle of  $\Delta\theta \sim 0.57^\circ$  or  $\sim 10$  mrad, this constitutes a substantial, almost two-orders of magnitude improvement allowing now for high resolution ( $\Delta\varepsilon \sim 100$  meV) electron spectra measurements at realistic count rates. At  $\theta = 0^\circ$ , where ZAPS measurements are performed (for details see the experimental setup section),  $\theta'$  can be either  $0^\circ$  or  $180^\circ$  (see Fig. 1) resulting in a corresponding addition or subtraction of velocities. In this case, the resulting laboratory electron energy can be readily obtained from Eqs. 1 setting  $\theta' = 0^\circ$  or  $180^\circ$  to be:

$$\varepsilon_{\pm}(\theta = 0^\circ) = (\sqrt{\varepsilon'} \pm \sqrt{t_p})^2 \quad (3a)$$

or its more accurate relativistic counterpart

$$\varepsilon_{\pm}(\theta = 0^\circ) = \frac{1}{2} \left[ \sqrt{(1 + \gamma_p)\varepsilon'} \pm \sqrt{(1 + \gamma')t_p} \right]^2 \quad (3b)$$

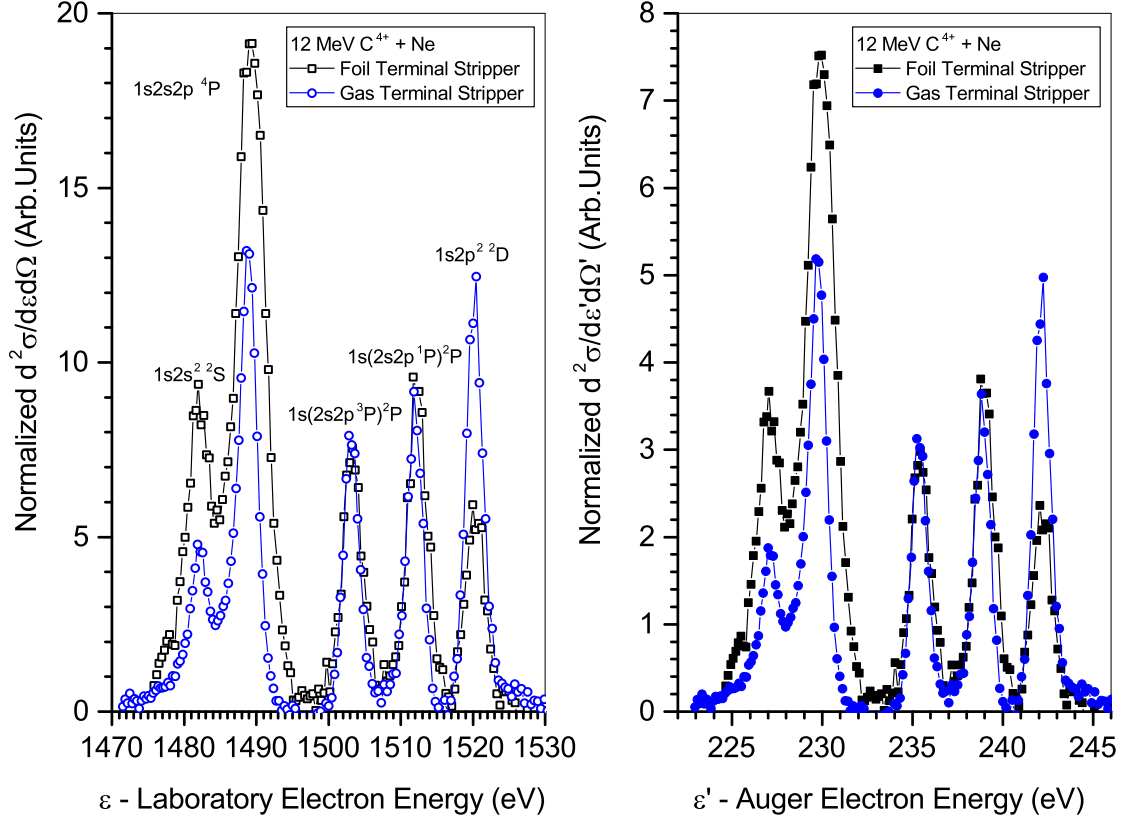


Figure 2. Typical ZAPS electron spectra obtained with our new apparatus at Demokritos for 12 MeV  $C^{4+}$  collisions with neon gas: (Left) Laboratory (open symbols) spectra, (Right) Projectile rest frame spectra. The spectra were obtained by foil stripping (black squares) or gas stripping (blue circles) the negative ion carbon beam in the terminal of the accelerator. As can be directly observed, the different stripping methods produce different ratios of  ${}^4P^o/{}^2D$  line intensities implying different amounts of pre-excited metastable fraction  $1s2s\ 3S$ . For the gas stripped spectra, the newly installed terminal gas stripper was used. The energy axes are related by Eq. 1, while the doubly differential cross section axes have been transformed according to Eq. 4.

In Fig. 2 we show typical high resolution zero-degree electron spectra, where the + sign in Eqs. 3 is applicable. The projectile lines corresponding to  $KLL$ -Auger transitions are well resolved. The particular states can be readily identified by comparison to atomic structure calculations<sup>6</sup>.

In addition to the transformation of the energy axis there is also a corresponding trans-

formation of the double differential cross section (DDCS) (the y-axis) such that:

$$\frac{d^2\sigma}{d\Omega'd\varepsilon'} = \sqrt{\frac{\varepsilon'}{\varepsilon}} \frac{d^2\sigma}{\varepsilon d\Omega d\varepsilon} \quad (4)$$

In the case of Fig. 2 since  $\varepsilon' < \varepsilon$ , the transformation to the rest frame of Eq. 4 shows that the spectra in the laboratory are relatively enhanced by the factor  $\sqrt{\frac{\varepsilon}{\varepsilon'}}$  which is an additional help to the experimenter.

### III. SINGLE-ELECTRON CAPTURE

In ion-atom collisions one of the more interesting processes that can be investigated is electron capture to excited atomic states (not to be confused with *nuclear* electron capture). In *single* electron capture, an electron is transferred from the target atom to the projectile ion. Exactly where and how this electron is transferred depends on the collision system investigated. The information about the transfer to excited states of the projectile can only be inferred spectroscopically by observing transitions (either radiative<sup>7,8</sup> or Auger<sup>9</sup>) from the excited atomic states to lower lying states. Recently, interest has focused on electron capture to pre-excited states of ions<sup>9-13</sup>, i.e. to collisions in which the incoming ion is already in some excited state. This allows for the investigation of excited states not readily producible in any other way. Thus, for example the spectra shown in Fig. 2, were obtained using two-electron  $C^{4+}$  ion beams in a mixture of pre-excited  $1s2s\ ^3S$  and  $1s^2$  ground states. The  $1s2s\ ^3S$  state is metastable (long-lived) since it can only decay by a forbidden spin changing transition. The  $1s2s\ ^3S$  state is produced in the ion stripper inside the tandem accelerator terminal together with the ground state ions in variable amounts 5-30% depending on the stripping medium (gas or foil) and stripping energy<sup>14,15</sup>. Capture to the ground state of the now Li-like ion formed, i.e.  $1s^22s$  cannot de-excite so it is not accessible spectroscopically. However, electron capture to the  $1s2s\ ^3S$  metastable state leads to a spectroscopically rich spectrum:



the excited states formed in the case of  $n = 2$  (according to electron spin-orbit coupling rules) are identified in the spectra of Fig. 2 from their characteristic Auger decay energies  $\varepsilon'_A$ :

$$\begin{aligned}
& C^{3+}[1s2s2\ell^{2S+1}L_J] \quad (L = \ell = 0, 1 \ S = 3/2, 1/2, \ \mathbf{J} = \mathbf{L} + \mathbf{S}) \\
& \quad \downarrow \\
& C^{4+}(1s^2) + e^-_A(\varepsilon'_A) \quad (6)
\end{aligned}$$

Thus, the production of the  $1s2s^2\ ^2S$  and  $1s2s2p\ ^{2,4}P$  lines observed in the Auger spectra can be readily produced by direct single  $2s$  or  $2p$  electron capture into the  $1s2s\ ^3S$  component of the ion beam.<sup>12,16</sup> However, the line labeled  $1s2p^2\ ^2D$  *cannot* be produced by single electron capture to the  $1s2s\ ^3S$  state since it requires an additional  $2s \rightarrow 2p$  excitation. In the energy range of these collisions another related *two*-electron process involving the transfer of a target electron to the  $2p$  orbital simultaneously with  $1s \rightarrow 2p$  excitation from the ground state is now quite probable. This process, known as transfer-excitation (TE)<sup>17,18</sup>, can also populate the other two  $^2P$  lines observed (through a  $2s$  transfer), but *not* the  $^4P$ . This again has to do with active spin selection rules which would require a low probability spin flipping TE transition to occur from the ground state. Therefore, according to our present understanding<sup>19</sup>, the  $^4P$  is produced *only* from the metastable state by direct single electron capture<sup>12,16</sup>, while the  $^2D$  line *only* from the ground state through the afore mentioned TE process.

Basic quantum mechanics require the spin coupling of the  $2p$  electron to the  $1s2s\ ^3S$  state yielding  $1s2s2p\ ^4P$  quartet and  $1s2s2p\ ^2P$  doublet states to be in the ratio of 2:1, i.e.  $R = \frac{\sigma(1s2s2p\ ^4P)}{\sigma(1s(2s2p\ ^3P)\ ^2P) + \sigma(1s(2s2p\ ^1P)\ ^2P)} = \frac{\sigma(1s2s2p\ ^4P)}{\sigma(1s2s2p\ ^2P)} = 2$ , where  $\sigma$  is the capture cross section into the particular state<sup>20</sup>. Thus, it came as a big surprise that the measured ratio  $R$ , was found to be closer to 10 for  $C^{4+}$  beams<sup>12</sup>, clearly calling for an explanation. A new two-electron process termed the *Pauli exchange interaction* was subsequently proposed<sup>12</sup>, where a target electron which is spin-aligned with the two projectile electrons in the  $1s2s\ ^3S$  state experiences a (slightly) different potential than an anti-aligned electron. If the interaction potentials are different, the outcomes ( $^4P$  vs.  $^2P$  formation) could also be different. This process does not necessarily involve the excitation of the projectile  $1s$  electron and could possibly be described within the independent electron model, but one would need spin-dependent potentials - a difficult task - not yet attempted<sup>21</sup>.

However, more recently it has also been shown that capture to higher lying ( $1s2snl^{2,4}L_J$ ) states should also be very probable and therefore *selective cascade feeding* of the  $1s2s2p^4P$  can also be expected to occur<sup>13,22,23</sup>. The  $^2P$  states Auger decay strongly to the K-shell, while the  $^4P$  quartets Auger decay much more weakly due to spin selection rules.  $E1$  transition rates, however, are the strongest for quartet to quartet and/or doublet to doublet transitions. This results in a selective cascade feeding mechanism directly enhancing the  $^4P$  populations.

Finally, the inherent long lifetime ( $\sim ns-\mu s$  depending on atomic number and  $J$ ) of the  $1s2s2p^4P_J$  (with the total angular momentum  $J = 1/2, 3/2, 5/2$  lines unresolved) metastable states leads to an additional difficulty in the quantitative analysis of the measured  $1s2s2p^4P$  production cross section<sup>16,22</sup>. In  $0^\circ$  measurements, the electron spectrometer lies in the direct path of the ion beam, and therefore the metastable projectile states decay all along the ionic projectile path towards and through the spectrometer. One therefore has to correctly take into account both the decay of these states along the path of observation and the increase of the spectrometer acceptance solid angle, as the emission point approaches the entry of the spectrometer. This can result in a considerable correction to the measured metastable electron yield. This correction has been treated in the literature, either in a purely geometrical approach<sup>16,22</sup> or very recently, for our measurements using an HDA with entry lens, in a Monte Carlo electron trajectory simulation approach within the well-known SIMION<sup>24</sup> charged particle optics software<sup>25</sup>. In this latter approach, kinematic effects, particular to Auger emission from fast moving projectile ions such as kinematic line broadening and solid angle limitations due to  $\theta_{max}$ , are also included for the first time, allowing for a more accurate and realistic line shape modelling<sup>25</sup> of both metastable and prompt Auger lines.

The APAPES project has embarked on an isoelectronic study of electron capture into  $1s2s^3S$  state of He-like ions to shed more light on these processes.

#### IV. ION BEAM STRIPPING CONSIDERATIONS - PRODUCTION OF PRE-EXCITED IONS

An important difference between nuclear and atomic physics is the interest in the *electron* structure of the ion beam and therefore its charge state. The charge state determines the number of electrons on the ion. Thus, for example a He-like ion like  $C^{4+}$  has two electrons,

while a Li-like ion like  $C^{3+}$  has three electrons. The number of electrons carried into the collision by the projectile is important since it also determines the resulting atomic state after the collision, depending on whether a net ionization, excitation or capture process takes place. Highly-charged ions typically carry just a few electrons resulting in more easily interpretable collision spectra which can provide more stringent tests of theory<sup>4</sup>.

The production of highly-charged ions is therefore of great interest in atomic collision physics. Such ions are typically produced by passing a low charge state beam through a thin foil or gas, where numerous electrons can be stripped from the ion, thus increasing its charge state. These strippers are found in the terminal of all tandem Van de Graaff accelerators since they are needed to convert the initially negatively charged ion beam to a subsequently positively charged beam which is further energy boosted in the second stage of acceleration. The desired charge state and energy are typically selected by the analyzing magnet and send on to the experiment. Depending on the energy of the ion beam during the stripping process, a particular gaussian-like charge state distribution results centered around the mean charge state. The higher the energy of the beam, the higher the mean charge state<sup>26-28</sup>. Thus, to produce more intense few-electron or even bare ion beams additional stripping points *after* the beam exits the accelerator are provided known as *post*-strippers.

We have recently installed such a set of post-strippers (both gas and foil) for use at the TANDEM between the analyzing magnet and the switching magnet. For example, Fig. 3 shows the expected relative amounts of  $O^{6+}$  beams that can be produced as a function of stripping energy both at the lower stripping energies inside the accelerator terminal by either foil or gas stripping and also at the higher stripping energy for either gas or foil *post*-stripping. As can be seen, the fraction of  $O^{6+}$  ions is rather low if one uses only the terminal strippers. However, combined with a post-stripper, the fraction increases, reaching a predicted maximum of  $\sim 25-30\%$  of the beam prior to stripping. These type of charts are produced with the help of stripping codes which apply a set of empirical equations<sup>26,27</sup>, to predict the resulting charge distributions, thus allowing the experimenter to select the most efficient way to obtain the desired energy and ion species with sufficient intensity to perform the required measurement.

An additional requirement of the APAPES project is to also have a variable (and controllable) amount of metastable beam component ( $1s2s\ ^3S$ ). To date, there are no codes that can generally predict the fraction of metastable ions. However, previous studies have shown

that the amount of metastables varies mainly depending on whether a foil or a gas stripper is used, with the metastable amount typically reaching a maximum of  $\sim 30\%$ , when using a foil stripper. We have recently, also installed a gas terminal stripper inside the TANDEM which produces the He-like beam predominantly in the ground state. By performing two different measurements with beams of appreciably different metastable fractions, we can extract the contributions from either the ground state or the metastable state in the production of the  $^2P$  lines in the spectrum and therefore determine the electron capture ratio  $R$  of interest. This technique is presented in detail in a recent publication<sup>19</sup>. The installed gas terminal stripper uses a turbomolecular pump to differentially pump the stripping canal, thus preventing the contamination of the accelerator tube vacuum, while at the same time re-circulating and re-using the stripper gas. An additional advantage of the gas strippers is that they do not suffer damage, as do the foils, particularly at the lower stripping energies. Of added interest for ZAPS measurements, the ions lose less energy in the gas stripping medium compared to the foil as energy straggling is smaller<sup>29</sup>, thus producing stripped ion beams with a narrower energy distribution than those produced by foil stripping. Because measured electrons come from the moving ion, the effect of the ion's energy distribution can be seen in the broadening of the observed projectile Auger lines, particularly when measured with high electron energy resolution.

## V. EXPERIMENTAL SET UP AND RESULTS

The experimental setup of APAPES is housed in a dedicated beam line (L45 in the red room of the TANDEM measurement halls) for atomic collision physics and is shown in Fig. 4. The mixed state  $C^{4+}$  ion beam supplied by the TANDEM at energies ranging from  $\sim 6$ -18 MeV is directed into a doubly differentially pumped gas cell where it collides with the target gas. With this system a stable analyser chamber vacuum of  $\sim 10^{-6}$  Torr can be maintained for typical gas cell pressures in the mTorr range. The Auger electrons emitted at zero degrees with respect to the beam direction are analysed in energy with a maximum resolution  $\frac{\Delta E}{E} \sim 0.1\%$  using an electrostatic paracentric<sup>31-35</sup> hemispherical deflector analyser (HDA) equipped with a 4-element focusing/deceleration entry lens and a 2-dimensional position sensitive detector (PSD)<sup>36,37</sup>. Since the energy resolution is fixed by the spatial characteristics of the analyser, higher absolute resolution  $\Delta E$  is achieved by pre-retarding

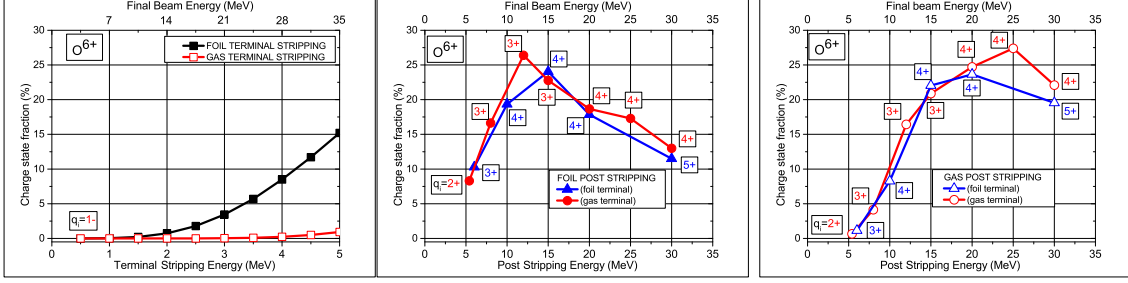


Figure 3. Fraction (in %) of the stripped oxygen beam which results in the final charge state of  $O^{6+}$  plotted as a function of the stripping energy as predicted by the TARDIS code<sup>30</sup> assuming 100% transmission. (Left) Terminal (T) Stripper: foil or gas, (Middle) Post (P) stripper: foil, using either gas or foil T stripper, (Right) Post (P) stripper: gas, using either gas or foil T stripper. The numbers in the squares refer to the charge state of the primary oxygen beam before final stripping. The bottom x-axis refers to the stripping energy, while the top to the final beam energy after final stripping. Prior to the new strippers installation, only the terminal foil stripper existed (filled black squares). As an example, a beam of 20 MeV  $O^{6+}$  should be produced in the following relative amounts: (1) Only terminal (T) stripped in foil = 4% or (2) in gas <1%. The availability of the post-strippers (P) allows the following 4 additional combinations: (3) foil(P) - foil(T) = 18%, (4) foil(P) - gas(T) = 19%, (5) gas(P) - foil(T) = 24%, (6) gas(P) - gas(T) = 25%. The stripping combination best suited to the experimental application can then be readily selected.

the Auger electrons. This is enough to resolve the Li-like K-Auger lines presented here. Finally, the analysed electron spectra are normalized to the number of ions collected in the FC2 Faraday Cup located at the exit after the HDA (see Fig. 4).

Following the successful installation and testing of both terminal gas stripper and foil/gas post-strippers, we have been able to obtain Auger spectra with variable amounts of metastable beam fraction as already shown in Fig. 2. Once we have better quantified the value of the metastable fraction in the delivered beam, we shall apply a new technique recently developed for the accurate determination of the electron capture ratio  $R$  [19]. First measurements at 12 MeV are encouraging and show sufficient proximity to the values of  $R$  predicted by theory and seem to support the selective cascade feeding model.

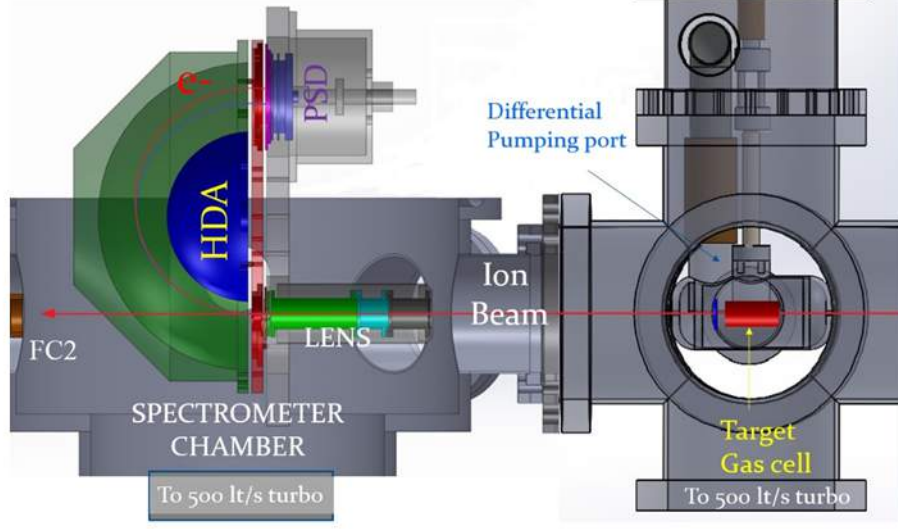


Figure 4. Our experimental setup consists (from right to left) of a doubly differentially pumped target gas cell, a 4-element entry lens, a large hemispherical deflector analyser (HDA) with 40 mm diameter 2-D position sensitive detector (PSD). The length of the target gas cell is  $L_c = 49.9$  mm and the distance of its center to the lens entry  $s_0 = 288.5$  mm.

## VI. SUMMARY AND CONCLUSIONS

We have presented the basics of the Zero-degree Auger Projectile Spectroscopy (ZAPS) technique used at the new beam line dedicated to atomic collisions physics at the Demokritos TANDEM. This unit is now in operation and can perform high energy resolution Auger electron spectroscopy of projectile ions excited during their collision with gas targets which allows for the state selective determination of differential cross sections. Details of the experimental setup were described with particular application to studies of single electron capture to He-like ions in the pre-excited  $1s2s^3S$  long-lived state. A terminal gas stripper along with both gas and foil post-strippers has also been installed in the TANDEM to be used to provide more intense He-like beams with variable amounts of  $1s2s^3S$  beam fraction. The new stripping systems can be utilized by all TANDEM users, to obtain more intense ion beams at energies and charge states not previously possible.

## VII. ACKNOWLEDGEMENTS

This work was co-financed during 2012-2015 by the European Union (European Social Fund ESF) and Greek national funds through the Operational Program “Education and Lifelong Learning” of the National Strategic Reference Framework (NSRF) Research Funding Program: THALES. Investing in knowledge society through the European Social Fund, grant number MIS 377289. It is a pleasure to acknowledge the help of various colleagues during the development of the entire experimental program over the last four years including Drs. Anastasios Dimitriou, Bela Sulik and Ivan Valastyan of the ATOMKI Institute in Debrecen Hungary, Omer Sise, Genoveva Martinez, Theo Mertzimekis, students Tasos Kanelakopoulos, Myrto Asimakopoulou, Christos Nounis, accelerator engineer and operator Miltos Andrianis, as well as David Manura of Scientific Instrument Services for help with SIMION Lua programming. Last, but not least, we thank the director of INPP, Dr. Sotiris Harissopulos, for his enthusiastic encouragement and support through out the entire program.

## REFERENCES

- <sup>1</sup><http://apapes.physics.uoc.gr/>.
- <sup>2</sup>I. Madesis *et al.*, J. Phys: Conf. Ser. **583**, 012014 (2015).
- <sup>3</sup>A. Dimitriou *et al.*, J. Atom. Mol. Cond. Nano Phys. **3**, 125 (2016).
- <sup>4</sup>T. J. M. Zouros and D. H. Lee, in *Accelerator-based atomic physics techniques and applications*, edited by S. M. Shafroth and J. C. Austin (American Institute of Physics Conference Series, Woodbury, NY, 1997), Chap. 13, pp. 426–479.
- <sup>5</sup>N. Stolterfoht, Physics Reports **146**, 315 (1987).
- <sup>6</sup>R. Bruch, K. T. Chung, W. L. Luken, and J. C. Culberson, Phys. Rev. A **31**, 310 (1985).
- <sup>7</sup>M. Druetta, S. Martin, and J. Desesquelles, Nucl. Instrum. Methods Phys. Res. B **23**, 268 (1987).
- <sup>8</sup>S. Bliman, M. Cornille, and K. Katsonis, Phys. Rev. A **50**, 3134 (1994).
- <sup>9</sup>E. P. Benis *et al.*, J. Phys. B **36**, L341 (2003).
- <sup>10</sup>M. Zamkov *et al.*, Phys. Rev. A **65**, 032705 (2002).
- <sup>11</sup>E. P. Benis *et al.*, Phys. Rev. A **69**, 052718 (2004).

- <sup>12</sup>J. A. Tanis *et al.*, Phys. Rev. Lett. **92**, 133201 (2004).
- <sup>13</sup>T. J. M. Zouros, B. Sulik, L. Gulyas, and K. Tokesi, Phys. Rev. A **77**, 050701 (2008).
- <sup>14</sup>M. Zamkov *et al.*, Phys. Rev. A **64**, 052702 (2001).
- <sup>15</sup>M. Zamkov, E. P. Benis, P. Richard, and T. J. M. Zouros, Phys. Rev. A **65**, 062706 (2002).
- <sup>16</sup>D. H. Lee *et al.*, Nucl. Instrum. Methods Phys. Res. B **56/57**, 99 (1991).
- <sup>17</sup>D. H. Lee *et al.*, Phys. Rev. A **44**, 1636 (1991).
- <sup>18</sup>T. J. M. Zouros, in *Recombination of Atomic Ions*, NATO Advanced Study Institute Series B: Physics, edited by W. G. Graham, W. Fritsch, Y. Hahn, and J. Tanis (Plenum Publishing Corporation, New York, 1992), Vol. 296, pp. 271–300.
- <sup>19</sup>E. P. Benis and T. J. M. Zouros, J. Phys. B **49**, 235202 (2016).
- <sup>20</sup>E. P. Benis *et al.*, Phys. Rev. A **73**, 029901 (2006).
- <sup>21</sup>T. Kirchner, 2016, private communications.
- <sup>22</sup>D. Strohschein *et al.*, Phys. Rev. A **77**, 022706 (2008).
- <sup>23</sup>D. Röhrbein, T. Kirchner, and S. Fritzsche, Phys. Rev. A **81**, 042701 (2010).
- <sup>24</sup>D. Manura, *Simion® Version 8.0/8.1 User Manual*, Scientific Instrument Services, Inc, 1027 Old York Rd, Ringoes, NJ 08551, 2011.
- <sup>25</sup>S. Doukas *et al.*, Rev. Sci. Instrum. **86**, 043111 (2015).
- <sup>26</sup>H.-D. Betz, Rev. Mod. Phys. **44**, 465 (1972).
- <sup>27</sup>Sayer, R.O., Rev. Phys. Appl. (Paris) **12**, 1543 (1977).
- <sup>28</sup>A. Laoutaris *et al.*, J. Phys: Conf. Ser. **635**, 052062 (2015).
- <sup>29</sup>P. Hvelplund, Phys. Rev. A **11**, 1921 (1975).
- <sup>30</sup>E.-M. Asimakopoulou *et al.*, poster presentation at HNPS (unpublished).
- <sup>31</sup>E. P. Benis and T. J. M. Zouros, Nucl. Instrum. Methods Phys. Res. A **440**, 462 (2000).
- <sup>32</sup>T. J. M. Zouros and E. P. Benis, J. Electron Spectrosc. and Relat. Phenom. **142**, 175 (2005).
- <sup>33</sup>E. P. Benis and T. J. M. Zouros, J. Electron Spectrosc. and Relat. Phenom. **163**, 28 (2008).
- <sup>34</sup>O. Sise *et al.*, J. Electron Spectrosc. and Relat. Phenom. **177**, 42 (2010).
- <sup>35</sup>M. Dogan, M. Ulu, G. G. Gennarakis, and T. J. M. Zouros, Rev. Sci. Instrum. **84**, 043105 (2013).
- <sup>36</sup>E. P. Benis *et al.*, Nucl. Instrum. Methods Phys. Res. B **146**, 120 (1998).
- <sup>37</sup>E. P. Benis, T. J. M. Zouros, and P. Richard, Nucl. Instrum. Methods Phys. Res. B **154**, 276 (1999).